



THERMOELECTRIC, RESISTANCE, PHOTO ELECTRIC DETECTORS AND ANALYSIS OF SPECTRAL CHARACTERISTICS OF MATERIALS IN THEM

Mamirov Abduvoxid Muxammadamin o'g'li

Andijan Machine Building Institute

Tel: (+99899) 326-66-47 E-mail: mamirov_1991@inbox.ru

Kodirov Sardorbek Anvar o'g'li

Andijan Machine Building Institute

Tel: (+99899) 326-66-47 E-mail: mamirov_1991@inbox.ru

Annotation

The conversion of light photons into some measurable signal is the goal of radiometric detectors. Historically, there have been several tools to accomplish this conversion. This includes the introduction of photoelectric effects for thermal processes and solid state detectors. Thermal processes include calorimetry and thermoelectric effects. This article describes the operating technology and types of detectors and explains the spectral characteristics of thermoelectric materials.

Keywords: Thermoelectric detectors, thermojunction, thermocouple, Resistance Detectors, thermistor, Photoelectric detectors, Pyrheliometers, Circumsolar radiation, Spectral distributions, solar energy

THERMOELECTRIC DETECTORS

Thermopiles

A thermoelectric signal is produced by the Seebeck effect [4,5]. An electric potential (voltage) is produced when a "thermojunction" (called a thermocouple) is the result of dissimilar metals in contact with each other and in thermal contact with an absorber. A difference in temperature between the sensing junction thermocouple (sensed as the temperature of the absorber) and an identical thermocouple at a reference temperature is required to generate the thermoelectric voltage. Different dissimilar metal combinations are identified as different thermocouple "types." Each thermocouple type produces a different thermoelectric voltage per degree of temperature difference between the reference and sensing junctions. The relationship between the thermoelectric voltage and temperature is also a function of the temperature difference. Over relatively small temperature ranges (about 100°C or 100 K), the voltage/temperature relationship can be considered approximately linear [6].





A commonly used combination is the type T thermocouple, consisting of junctions of copper and constantan. In the range of temperatures encountered in solar radiometers (-40°C to $+50^{\circ}\text{C}$) and temperature differences developed by black absorbing sensors (about 5°C), the type T thermocouple produces about 40 microvolts per degree centigrade ($\mu\text{V}/^{\circ}\text{C}$) [6]. To increase the signal to a magnitude that can be measured accurately and reliably, thermojunctions are connected together in series to build a thermopile. The thermopile voltage is directly proportional to the number of junctions in the thermopile. Thus, for a 40-junction type T thermopile in contact with an absorber 5°C warmer than the reference junctions, the expected output voltage is $40 \times 40 \mu\text{V}/^{\circ}\text{C} \times 5^{\circ}\text{C} = 8000 \mu\text{V}$ or 8 millivolts (mV). This is a reasonable voltage for measurement by modern electronic equipment. Precision miniature thermopiles such as used in solar radiometers are relatively expensive, and the radiometer requires careful design to incorporate the reference junctions, an efficient thermal absorber, protection from the environment for the sensing and reference junctions, and so on.

Resistance Detectors

Another thermoelectric property sometimes used is the resistance temperature detector (RTD). This measurement approach relies on the change in resistance of certain materials as a function of temperature. Platinum is the most common example, thus there are platinum resistance temperature detectors (PRTDs). Platinum has a temperature coefficient of 0.358% per degree centigrade. The resistance of the detector element is determined by measuring the voltage drop across the sensor when a known current is passed through the sensor. This is a straightforward application of Ohm's law: $R = V/I$, where V = voltage (volts), I = current (amperes), and R = resistance (Ohms). However, this approach has the disadvantage of requiring a stable, accurately known current source and accurate resistance measurement equipment [7].

Another example of thermoelectric detectors, rarely used in solar radiometry, is the thermistor. This detector is similar to the RTD in that the temperature coefficient of resistance (TC) is very large. These detectors are often used for ambient temperature and in laboratory temperature measurement and monitoring equipment. A common thermistor temperature coefficient is in ohms per degree centigrade. In this case, the thermistor TC is not a linear function of the resistance itself but a logarithm of the resistance. A common method of converting the resistance to temperature is the Steinhart–Hart equation [8]:



$$T = 1/(a + b(\ln R) + c(\ln R)^2 + d(\ln R)^3) \quad T = 1/(a + b(\ln R) + c(\ln R)^2 + d(\ln R)^3)$$

This measurement approach has the same disadvantages as the RTD, namely, an accurate and stable current source and resistance measurement instrumentation. In addition, the coefficients for Equation 2.1 must be derived individually for each thermistor using regression analysis of calibration temperatures versus resistance measurements. This means the statistical properties of the coefficients and overall scatter about the regression equation contribute to the uncertainty in the temperature estimate. Since the detector produces a temperature (or temperature difference measurement), this is essentially a calorimetric measurement technique.

Photoelectric Detectors

Einstein won the Nobel Prize in Physics in 1905 for explaining the generation of electric current by materials that were illuminated by photons [9]. Electrons in the atoms of the photoelectric material absorb energy proportional to the frequency, or wavelength, of the photons: $E = h\nu = hc/\lambda$, where h is Planck's constant ($6.62606957 \times 10^{-34}$ joule seconds or joule/hertz), λ is the wavelength of the photon or light (meters), ν is the frequency of the light (Hz), and c is the speed of light in a vacuum (2.999×10^6 km/s).

If the photon energy is great enough, the electrons absorb enough energy to escape their atomic orbits and move to the conduction band. That is, the electrons move freely about within the matrix of the material and can produce an electric current in an external circuit. The "gap" between the energy keeping the electrons bound to the atom and the conduction band is called the band gap of the material [10]. Photons with energy greater than the band gap (typically measured in electron volts, eV) are absorbed and provide enough energy to produce free electrons in the material. The relation between energy, in terms of electron volts and photon wavelength (or frequency), is

$$E = h\nu \quad E = hc/\lambda \quad (2.2)$$

The relationship between the material band gap and distribution of the wavelengths of light (spectral distribution) hitting the material means that the material will produce free electrons only for photons with a limited wavelength range.





This is called the spectral response region of the detectors. The most common solid-state detector used on solar radiometers is crystalline silicon, with a band gap of 1.1 eV. This means photons of wavelength greater than about 1 micrometer (μm) or 1000 nanometer (nm) cannot produce conduction band electrons. Various other materials, including various forms of silicon, such as “metallurgical-grade,” multicrystalline, or amorphous silicon, have widely differing spectral response functions that not discussed here.

Silicon detectors are relatively inexpensive and have several disadvantages that affect their accuracy in solar radiometry. First is the limited spectral response region (about 75% of the total solar spectrum. The spectral distribution of sunlight is highly variable, and certain parts of the solar spectrum where the variability is high are not sensed by the silicon detector. Thus, information about the variability in the spectrum outside the spectral response region is not contained in the sensor signal.

Second, the signal the detector produces is an electron current. Third, this signal can be relatively small, a few tens of microamperes (μA) per incident unit of power (Wm^2). Measurement of current directly is usually less accurate than measurements of voltage. To get a voltage signal that can be measured more accurately, a stable, low temperature coefficient resistor in parallel with the detector can be used. However, this is another component with quality that has an impact on the quality of the measurement. Last, silicon has a variable temperature coefficient of response, which is a function of the wavelength of light.

In the following sections, the issues associated with thermopile and silicon detector radiometers in radiometers for measuring solar irradiance components are discussed.

Pyrheliometers: Measuring Direct Normal Irradiance

Pyrheliometer Design

Measuring the direct normal irradiance (DNI) requires an instrument that collects all the photons in the beam, or solid angle, subtended by the solar disk (approximately 0.5° total solid angle, or 0.008 radians, about 10 milliradians [mR]), and blocking off photons from the rest of the hemisphere. This is accomplished with a “Gershun tube” or long narrow tube with baffles that limit the field of view (FOV) of the detector. The detector is placed at the bottom of the tube. The tube blocks off the sky diffuse photons. When the detector/tube combination is pointed at the sun (detector normal to the direct beam), only the photons in the FOV determined by the geometry of the tube length, baffles, apertures, and detector size are captured by the detector. This



device is called a pyr heliometer. The basic geometry of the tube, baffles, and detector to determine FOV are shown in Figure 1 [11].

A requirement for pyr heliometric measurements of the DNI is that the detector always be normal to the direct beam, which means the pyr heliometer must track the sun along its diurnal path throughout the day. Because the DNI beam is rather slender and small, the tracking accuracy requirements needed to ensure that all the photons in the beam get to the detector are very stringent. To reduce the tracking accuracy requirements (as well as the length of tube required to get the desired FOV), the FOV is generally opened up to a larger solid angle. This permits some tracking inaccuracy without losing photons from the beam.

Circumsolar Radiation

For a pyr heliometer with a larger FOV, part of the sky around the sun is also in the FOV of the detector. This region between the limb (edge) of the solar disk and the edge of the FOV is the circumsolar region and contains circumsolar radiation. At first, this circumsolar radiation may seem to introduce an error into the measurement of the DNI. This is not the case because the circumsolar radiation is radiation scattered out of the beam in random directions and is not collected by the pyr heliometer sensor [12].

The direction a scattered photon follows depends on the complex physics of the air molecules and other (variable) components in the atmosphere [10]. There may be some (usually small) part of the radiation scattered in the forward direction along the DNI beam. Direct measurements of the relative intensity or magnitude of the circumsolar radiation show that within a few arc seconds of the edge of the solar disk, the number of photons (magnitude of the intensity) falls off more than two or three orders of magnitude (factor of 1/100 to 1/1000) below the disk intensity [13,14]. Even if these forward-scattered photons reach the detector, they are “lost in the noise” or random thermal signal from the detector. The requirement for the number of circumsolar photons to exceed the signal-to-noise level is that the atmosphere contain a large number of scattering centers (particles) with sizes on the order of, or greater than, the wavelengths of light present in the solar spectrum. The theory of such scattering is due to Gustav Mie (1908) [15,16]. These conditions result in very large circumsolar regions and indistinct edges of the solar disk.



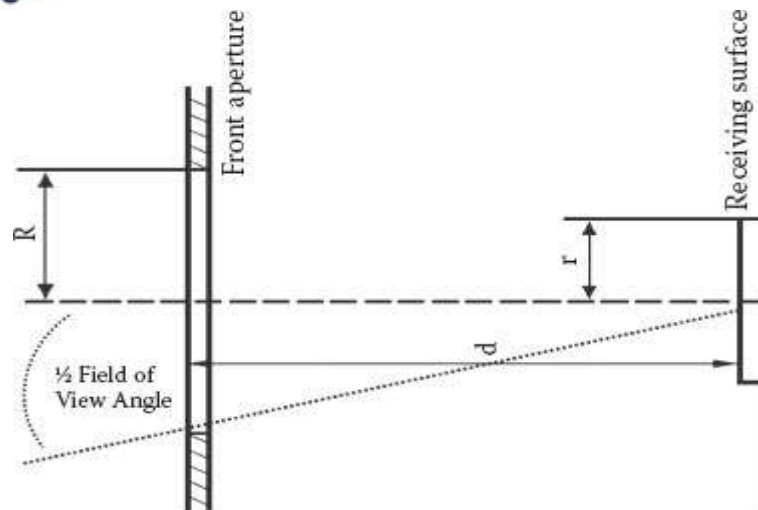


FIGURE 1 Field of view defining parameters for pyrhelimeters. (Adapted from World Meteorological Organization. 2008. WMO Guide to Meteorological Instruments and Methods of Observation, WMO No. 8, 7th ed. World Meteorological Organization, Geneva, Switzerland. http://www.wmo.int/pages/prog/gcos/documents/gruanmanuals/CIMO/CIMO_Guide-7th_Edition-2008.pdf. Accessed 21 July 2012.)

Spectral Distributions

Electromagnetic emissions from the sun extend across the electromagnetic spectrum from the highly energetic x-ray region through the ultraviolet, visible, and IR portion of the spectrum to the far IR and radio region. These emissions interact with Earth's own electromagnetic and atmospheric envelope, resulting in large variations in the magnitude of solar radiation available for conversion into other forms of useful energy. Most solar energy conversion systems utilize only part of the solar spectrum. For example, in lighting, [2] the energy in the human visual response range (wavelengths of 380 to 850 nm) are important. Crystal silicon photovoltaic cells convert radiation from 350 to 1100 nm, and plants use photosynthetically active radiation (PAR) between 400 and 700 nm [17]. However, the efficiency and performance of these systems are usually based on the total solar broadband radiation measured between 250 and 2500 nm. Specialized instruments and measurement techniques have been developed to quantify the available broadband solar resource and for spectral regions utilized by each technology, shown at the top of Figure 2. The spectra in Figure 2, [1] except for the extraterrestrial example, are only single examples of each of the component spectra. The spectral distribution of each component changes as air mass changes and as the constituents of the atmosphere change. [3]

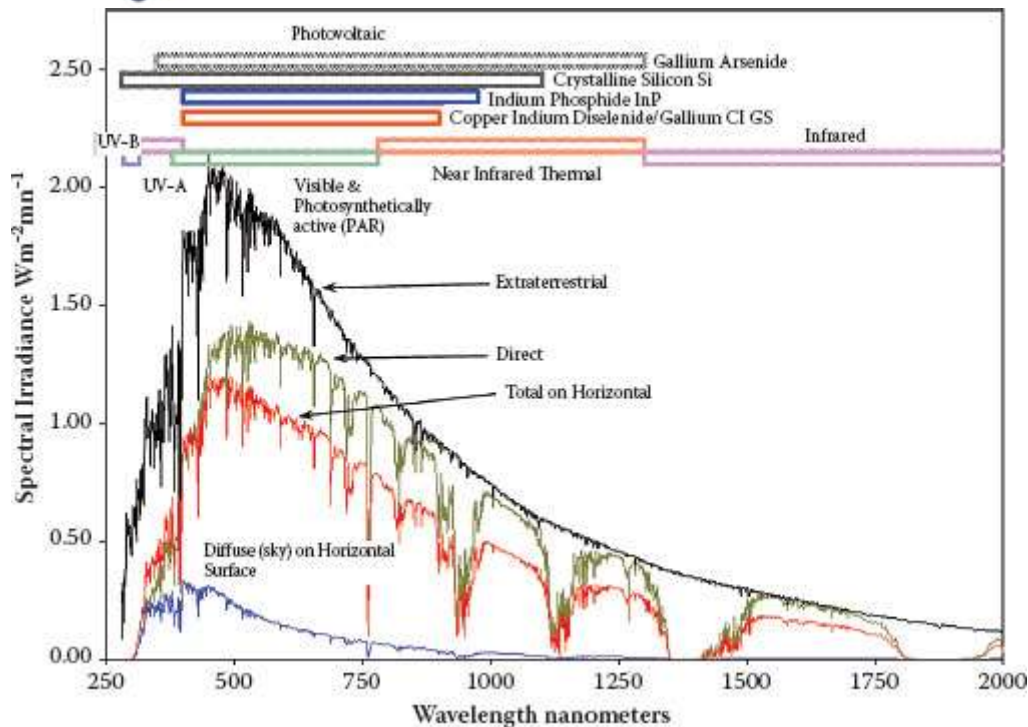


FIGURE 2 (See color insert.) Representative distributions of power as a function of wavelength for solar energy at the top of the atmosphere (extraterrestrial), solar beam radiation, diffuse sky radiation, and total radiation on a horizontal surface for clear sky conditions. Bars show regions of energy utilization by conversion systems. Note especially the difference between the global and diffuse horizontal spectra.

Conclusion

There are many measurement principles and approaches in measuring solar radiation. These measurements are one of the least accurate physical measurements. While mass, electric current, and other similar physical quantities can be measured with the accuracy of parts, or even better, our best current instrument for solar measurements is 3 parts or 0.3% per thousand. not more accurate. Our best regular measurements are no more than a few parts per hundred. This is due to the difficulty in physically assembling the photons and converting them into an easily measured electrical or thermal signal. Qualitative measurements of solar radiation are rare. This is mainly due to tool costs, but also due to the labor expended on calibrating and maintaining and assembling the tools, evaluating, processing, and archiving the data. Although the quality of future civilization may depend on the balance of incoming and outgoing solar radiation, high-quality measurements are less common around the world. The engineering of solar power systems based on these measurements is fraught with growing uncertainty when less and lower quality measurements are used. Finally, when using calculated or modeled values of solar radiation to design a solar



energy conversion system, it should be remembered that no model is more accurate than the measurement data that can be used to develop or validate the model. The engineering of solar power systems based on these measurements is fraught with growing uncertainty when less and lower quality measurements are used. Finally, when using calculated or modeled values of solar radiation to design solar energy conversion systems, it should be borne in mind that no model is more accurate than the measurement data that can be used to develop or validate the model. The engineering of solar power systems based on these measurements is fraught with growing uncertainty when less and lower quality measurements are used. Finally, it should be borne in mind that when solar calculation or modeled values are used in the design of solar energy conversion systems, no model is more accurate than the measurement data that can be used to develop or validate the model.

References

1. Mamirov A.M. I.I.Anarboev, L.O.Olimov Renewable energy applications for spectral data and models. "Mechatronics and Robotics: Problems and Development Prospects" collection of scientific works of the international scientific-technical conference Andijan 30-31-mart, 2021-yil 71-74 bb
2. Mamirov A.M / Monocrystalline and polycrystalline semiconductor materials. International scientific-practical conference "Digital technologies, innovative ideas and prospects for their application in production" Andijan 2021-yil 179-181 pp
3. Mamirov A.M Kodirov S.A Possibilities and significance of the solar oven device for high temperatures operating in small laboratory conditions JournalNX- A Multidisciplinary Peer Reviewed Journal India 2020. 177-180pp
4. Seebeck, T.J. (1821). Ueber den magnetismus der galvenische kette. Abhandlungen der Koniglich Akadamie der Wissenschaften, Berlin, pp. 289–325.
5. Benedict, R. (1981). Fundamentals of Temperature, Pressure and Flow Measurements, 3rd ed. Wiley, Hoboken, NJ.
6. Burns, G.W., M. Scroger, G.F. Strouse, M.C. Croarkin, and W.F. Guthrie (1993). Temperature-Electromotive Force Reference Functions and Tables for the Letter-Designated Thermocouple Types Based on the ITS-90. NIST Monograph 175. U.S. Department of Commerce Technology Administration, National Institute of Standards and Technology, Gaithersburg, MD. See <http://srdata.nist.gov/its90/main/>. Accessed 21 July 2012.
7. Tew, W.L., and G.F. Strouse. (2001). Standard Reference Material 1750: Standard Platinum Resistance Thermometers, 13.8033 K to 429.7485 K. NIST Special





Publication 260–139. U.S. Department of Commerce Technology Administration, National Institute of Standards and Technology, Gaithersburg, MD.

8. Steinhart, I.S., and S.R. Hart. (1968). Calibration curves for thermistors. *Deep Sea Research*, Vol. 15, p. 497.

9. Einstein, A. (1905). On the thermodynamic theory of the difference in potentials between metals and fully dissociated solutions of their salts and on an electrical method for investigating molecular forces. *Annalen der Physik*, Ser. 4, 8, pp. 798–814.

10. Pankove, J. (ed.). (1971). *Optical Processes in Semiconductors*. Prentice Hall, Englewood Cliffs, NJ.

11. World Meteorological Organization. (2008). *WMO Guide to Meteorological Instruments and Methods of Observation*, WMO No. 8, 7th ed. Geneva, Switzerland. http://www.wmo.int/pages/prog/gcos/documents/gruanm_anuals/CIMO/IMO_Guide-7th_Edition-2008.pdf, Accessed 21 July 2012.

12. van de Hulst, H.C. (1957). *Light Scattering by Small Particles*. Wiley, New York.

13. Neumann, A., A. Witzke, S.A. Jones, and G. Schmitt. (2002). Representative terrestrial solar brightness profiles. *Journal of Solar Energy Engineering, Transactions of the ASME*, Vol. 124, p. 198.

14. Buie, D., and A.G. Monger. (2004). The effect of circumsolar radiation on a solar concentrating system. *Solar Energy*, Vol. 76, pp. 181–185.

15. Mie, G. (1908). Beiträge zur Optik trüber Medien, speziell kolloidaler Metallösungen. *Annalen der Physik*, Vol. 330, pp. 377–445.

16. Hecht, E. (2001). *Optics*, 4th ed. Addison-Wesley, Boston.

17. Biggs, W.W., A. R. Edison, J. D. Eastin, K.W. Brown, J.W. Maranville, and M.D. Clegg. (1971). Photosynthesis light sensor and meter. *Ecology*, Vol. 52, pp. 125–131.

